Unconventional superconducting symmetry in a checkerboard antiferromagnet studied via renormalized mean-field theory

Huai-Xiang Huang,[1,2] You-Quan Li,[1] Jing-Yu Gan,[3] Yan Chen,[4] and Fu-Chun Zhang[4,1]
[1]*Department of Physics, Zhejiang University, Hangzhou 310027, China*
[2]*Department of Physics, Shanghai University, Shanghai 200444, China*
[3]*Center for Advanced Study, Tsinghua University, Beijing 100084, China*
[4]*Department of Physics and Center of Theoretical and Computational Physics, The University of Hong Kong, Pokfulam Road, Hong Kong, China*
(Received 30 December 2006; published 23 May 2007)

We use a renormalized mean-field theory to study the Gutzwiller projected Bardeen-Cooper-Schrieffer states of the extended Hubbard model in the large U limit or the t-t'-J-J' model on a two-dimensional checkerboard lattice. At small t'/t, the frustration due to the diagonal terms of t' and J' does not alter the $d_{x^2-y^2}$-wave pairing symmetry, and the negative (positive) t'/t enhances (suppresses) the pairing order parameter. At large t'/t, the ground state has an s-s wave symmetry. At the intermediate t'/t, the ground state is $d+id$ or $d+is$ wave with time reversal symmetry broken.

DOI: 10.1103/PhysRevB.75.184523 PACS number(s): 74.20.Rp, 74.25.Dw

I. INTRODUCTION

Geometrically frustrated systems with strong correlation have attracted much attention due to the highly nontrivial interplay between frustration and correlation.[1,2] In such systems, the pairwise interaction does not coincide with the geometry of the lattice, which may lead to exotic ground states. In particular, frustration in quantum magnets may cause certain types of magnetically disordered quantum phases, including the resonating valence bond (RVB) spin liquid state[3] and the valence bond crystal state.[4] The quantum spin liquid state could become unconventional superconducting state when the charge carriers are introduced. There have been experimental evidences for the unconventional superconductors in these systems. Examples are the triangular layer cobaltates compound Na_xCoO_2,[5] layered organic conductor κ-$(ET)_2Cu_2(CN)_3$,[6] the Kagome compound $SrCr_8Ga_4O_{19}$,[7] and three-dimensional (3D) beta-type transition-metal pyrochlore material KOs_2O_6.[8,9]

To describe the interplay between frustration and correlation, we consider a t-t'-J-J' model on a two-dimensional (2D) checkerboard lattice and analyze the possible superconducting pairing symmetry of the model. The checkerboard lattice is a frustrated one and may be considered as a 2D projection of a 3D corner-sharing lattice of pyrochlore. A schematic checkerboard lattice is illustrated in Fig. 1. The Hamiltonian reads

$$H = -\sum_{\langle ij\rangle\sigma} t_{ij} P_D (c^{\dagger}_{i\sigma} c_{j\sigma} + \text{H.c.}) P_D + \sum_{\langle ij\rangle} J_{ij} \vec{S}_i \cdot \vec{S}_j - \mu \sum_{i\sigma} c^{\dagger}_{i\sigma} c_{i\sigma}, \tag{1}$$

where $c^{\dagger}_{i\sigma}$ is an electron creation operator with spin σ at site i, $\vec{S}_i$ is a spin operator for electron, μ is the chemical potential, and $\langle ij\rangle$ denotes a neighboring pair on the lattice. P_D is a Gutzwiller projection operator to impose no double electron occupation at any site on the lattice. t_{ij} and J_{ij} stand for the hopping integrals and antiferromagnetic exchange couplings, respectively, and $t_{ij}=t$, $J_{ij}=J$ for the nearest neighbor (nn) links and $t_{ij}=t'$, $J_{ij}=J'$ for the diagonal or the next nn links, as shown in Fig. 1. For convenience, we use x,y to represent the nn links while a,b describe the two diagonal links. The Hamiltonian may be viewed as a strong coupling limit of a Hubbard model on the lattice with nn and next nn hopping integrals t and t', respectively, and an on-site Coulomb repulsive interaction U. Hereafter, we use t as an energy unit and set $J/t=1/3$. We choose $J'/J=(t'/t)^2$, consistent with the superexchange relation of $J=4t^2/U$ in the large U limit of the Hubbard model.

The model has certain limiting cases. At $t'/t\to 0$, the model is reduced to the t-J model on a square lattice. At $t'/t\to\infty$, the model becomes a collection of independent one-dimensional (1D) t'-J' chains. At $t'/t=1$, it is an isotropic checkerboard lattice with a highly geometrically frustrated structure.

Previous theoretical investigations mainly focused on the half-filled case without charge carriers. A variety of techniques have been employed to study the quantum antiferromagnetism on such a lattice.[10–14] Various quantum paramagnetic ground states may appear, which include some translational symmetry breaking states and a quantum spin

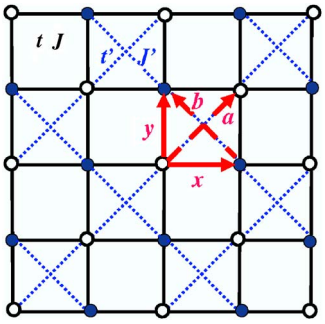

FIG. 1. (Color online) Schematic structure of 2D checkerboard lattice. Solid (open) circles represent sublattice A (B). The hopping integral and spin-spin coupling are t and J for the nearest neighbor links (solid lines) and t' and J' for the diagonal or next-nearest neighbor links (dashed lines), respectively.

liquid state. The introduction of doping with mobile charge carriers in a frustrated quantum antiferromagnet may result in the appearance of unconventional superconductivity.[15–19] Generally speaking, geometric frustration may play a key role in the mechanism of unconventional superconductivity. Recently, exact diagonalization approaches have been employed to study the superconducting fluctuations in this system with $t'=t$ and $J'=J$.[20–22] They found evidence of enhancement in pairing amplitude at arbitrarily small J/t for a specific sign of the hopping amplitude.

In this paper, we apply the plain vanilla version of the RVB theory[23,24] to study the ground state of the t-t'-J-J' model on a 2D checkerboard lattice. The competition among various superconducting states will be examined. Since our primary interest is on the possible pairing symmetry of the superconducting state for the doped system, we will not consider the possible long-range magnetic ordering in the present paper. Our main results can be summarized below. The $d_{x^2-y^2}$-wave pairing found for the t-J model extends to a large region in parameter space of t'/t and doping concentration δ, and the negative t'/t enhances the pairing while the positive t'/t suppresses the pairing. At small doping and for $|t'/t| \sim 1$, there is a small region where the pairing symmetry is $d+id$ or $d+is$. At $|t'/t| > 1$, there are regions where the pairing symmetry belongs to an s-s wave.

The rest of the paper is organized as follows. In Sec. II, we apply the renormalized mean-field theory to study the RVB state. In Sec. III, we present our numerical results on the possible superconducting ground states. In particular, four distinct superconducting phases show up in the phase diagram as a function of t'/t and the doping δ. Section IV is a summary. The diagonalization of the mean-field Hamiltonian and the explicit form of the self-consistent equations are presented in the Appendix.

II. FORMALISM

We use a Gutzwiller projected Bardeen-Cooper-Schrieffer (BCS) state[3] as a trial wave function to study the ground state and the corresponding pairing symmetry of Hamiltonian (1). The trial wave function is of the form

$$|\Psi_{GS}\rangle = \prod_i (1 - n_{i\uparrow} n_{i\downarrow}) |\Psi_{BCS}\rangle, \tag{2}$$

where $n_{i,\sigma}=c^\dagger_{i,\sigma}c_{i,\sigma}$, and the projection operator $\Pi_i(1-n_{i\uparrow}n_{i\downarrow})$ removes the doubly occupied electron states on every lattice site i. We use a renormalized mean-field theory[23,24] to calculate the energy of Hamiltonian (1). In the renormalized mean-field theory, we adopt the Gutzwiller approximation to replace the projection by a set of renormalized factors, which are determined by statistical countings.[25,26] We have

$$\langle c^\dagger_{i\sigma} c_{j\sigma}\rangle = g_t \langle c^\dagger_{i\sigma} c_{j\sigma}\rangle_0, \quad \langle \vec{S}_i \cdot \vec{S}_j\rangle = g_s \langle \vec{S}_i \cdot \vec{S}_j\rangle_0, \tag{3}$$

where g_t and g_s are the Gutzwiller renormalized factors and are given by[23] $g_t=2\delta/(1+\delta)$ and $g_s=4/(1+\delta)^2$, where δ denotes the doping density. Therefore, the variational calculations of H of Eq. (1) in the projected BCS state is reduced to the variational calculations of an effective Hamiltonian H_{eff} given below in the unprojected BCS states $|\Psi_{BCS}\rangle$ for H_{eff},

$$H_{eff} = \sum_{\langle ij\rangle\sigma} -g_t t_{ij}(c^\dagger_{i\sigma}c_{j\sigma} + \text{H.c.}) + \sum_{\langle ij\rangle} g_s J_{ij} \vec{S}_i \cdot \vec{S}_j - \mu \sum_{i\sigma} n_{i\sigma}. \tag{4}$$

To proceed further, we introduce particle-particle and particle-hole mean fields ($\tau = \pm\hat{x}, \pm\hat{y}, \pm\hat{a}, \pm\hat{b}$, see Fig. 1),

$$\Delta_\tau = \langle c^\dagger_{i\uparrow} c^\dagger_{i+\tau\downarrow} - c^\dagger_{i\downarrow} c^\dagger_{i+\tau\uparrow}\rangle_0,$$

$$\xi_\tau = \sum_\sigma \langle c^\dagger_{i\sigma} c_{i+\tau,\sigma}\rangle_0. \tag{5}$$

Here, we focus on the translational invariant state with the spin singlet and even parity superconducting pairing symmetry, where $\Delta_{i,i+\tau}=\Delta_{i+\tau,i}=\Delta_\tau$ and $\xi_{i,i+\tau}=\xi_\tau$. The superconducting order parameter is a 2×2 matrix representing the two sublattices,

$$\Delta_{SC}(\vec{k}) = \begin{pmatrix} \langle c^\dagger_{\vec{k}\uparrow A} c^\dagger_{-\vec{k}\downarrow A}\rangle & \langle c^\dagger_{\vec{k}\uparrow A} c^\dagger_{-\vec{k}\downarrow B}\rangle \\ \langle c^\dagger_{\vec{k}\uparrow B} c^\dagger_{-\vec{k}\downarrow A}\rangle & \langle c^\dagger_{\vec{k}\uparrow B} c^\dagger_{-\vec{k}\downarrow B}\rangle \end{pmatrix}. \tag{6}$$

Within the Gutzwiller approximation, it is related to Δ_τ by

$$\Delta_{SC}(\vec{k}) = g_t \begin{pmatrix} \Delta_a \cos k_a & \Delta_x \cos k_x + \Delta_y \cos k_y \\ \Delta_x \cos k_x + \Delta_y \cos k_y & \Delta_b \cos k_b \end{pmatrix}, \tag{7}$$

in the limit of $\delta=0$, consistent with the fact that the ground state is a Mott insulator at half-filling. At small δ, we have $\Delta_{SC}(\vec{k}) \sim \delta$.

In terms of these mean fields, the effective Hamiltonian can be expressed as

$$H_{MF} = \sum_{\langle ij\rangle\sigma} -\frac{3}{8} g_s J_{ij} (\xi_{ij} c^\dagger_{i\sigma} c_{j\sigma} + \Delta_{ij} c_{i\sigma} c_{j\bar{\sigma}} + \text{H.c.}) - g_t t_{ij} (c^\dagger_{i\sigma} c_{j\sigma} + \text{H.c.}) - \mu \sum_{i\sigma} n_{i\sigma} + \text{const.} \tag{8}$$

There are eight independent complex mean-field parameters: ξ_x, ξ_y, Δ_x, and Δ_y on the nn links and ξ_a, ξ_b, Δ_a, and Δ_b on the next nn links. Here, we assume all the particle-hole mean fields ξ to be real. We denote $\theta_{x,y}$, $\theta_{a,b}$, and $\theta_{x,a}$ as the relative phases of (Δ_x,Δ_y), (Δ_a,Δ_b), and (Δ_x,Δ_a), respectively. The energy per site can be expressed in terms of the mean fields and is given by

$$E_{gs} = -2g_t t(\xi_x + \xi_y) - g_t t'(\xi_a + \xi_b) - \frac{3}{8} g_s J(\xi_x^2 + \xi_y^2 + |\Delta_x|^2 + |\Delta_y|^2) - \frac{3}{16} g_s J'(\xi_a^2 + \xi_b^2 + |\Delta_a|^2 + |\Delta_b|^2). \tag{9}$$

The mean-field parameters ξ and Δ and the chemical potential μ can be determined by solving the self-consistent Eq. (5) together with an equation for the hole density. The mean-field state at zero temperature can be obtained by the diagonalization of H_{MF}. We then determine the lowest-energy state for each set of parameters t'/t and δ. The detailed formalism of the diagonalization of H_{MF} and the self-consistent equa-

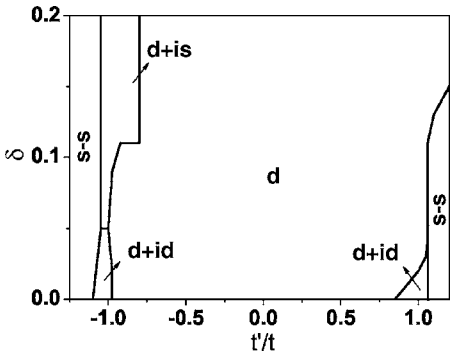

FIG. 2. Phase diagram of the t-t'-J-J' model on a checkerboard lattice in parameter space of hole density δ and t'/t obtained by the renormalized mean-field theory. The phases are indicated by their superconducting pairing symmetry defined in Table I and $J'/J=(t'/t)^2$.

tions can be found in the Appendix. These equations can be solved numerically, and the results are given in the next section.

III. NUMERICAL RESULTS

In this section, we present the numerical results of the self-consistent renormalized mean-field theory for Hamiltonian Eq. (1) on the checkerboard lattice. We will first discuss the phase diagram, then provide detailed analyses of the mean-field parameters as functions of δ for several typical values of t'/t. The phase diagram is shown in Fig. 2. The ground state at $\delta=0$ is a Mott insulator. At finite doping, the ground state is a superconducting state, with four different types of pairing symmetry, as illustrated in Table I. Here, we classify the pairing symmetry in terms of the relative phases between Δ_y and Δ_x, between Δ_b and Δ_a, and between Δ_a and Δ_x. Such a classification is consistent with the fourfold rotational symmetry in the Bravis lattice of the checkerboard structure.

At the limit $t'=J'=0$, the model is reduced to the t-J model, and the ground state has a $d_{x^2-y^2}$- or d-wave symmetry[23,27] at finite doping. This pairing state is robust against the next nn terms. As we can see from Fig. 2, the d-wave pairing symmetry of the ground state extends to a large region of both positive and negative values of t'/t. In such state, $\Delta_a=\Delta_b=0$, but there is an additional self-energy term arising from the next nn spin coupling. There are nodal

TABLE I. The pairing symmetries (shown in Fig. 2 and used in the text) of the ground states of the t-t'-J-J' model on a checkerboard lattice and their corresponding mean fields Δ_τ of Eq. (5). $\theta_{\tau,\tau'}$ are the relative phase between $\Delta_{\tau'}$ and Δ_τ.

Pairing symmetry	Mean-field parameters
d	$\Delta_x=-\Delta_y$, $\Delta_a=\Delta_b=0$
$d+id$	$\Delta_x=-\Delta_y$, $\Delta_a=-\Delta_b$, $\theta_{x,a}\approx\pi/2$
$s-s$	$\Delta_x=\Delta_y$, $\Delta_a=\Delta_b$, $\theta_{x,a}=\pi$
$d+is$	$\Delta_x=-\Delta_y$, $\Delta_a=\Delta_b$, $\theta_{x,a}\approx\pi/2$

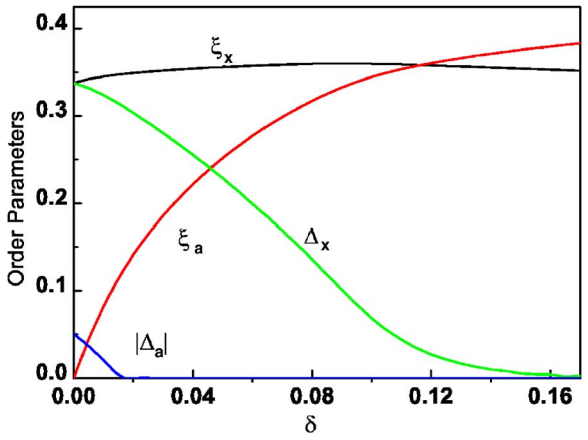

FIG. 3. (Color online) Amplitudes of mean fields ξ and Δ as functions of hole density δ for parameters $t=t'=1$, $J=J'=1/3$. The ground state has $d+id$ pairing (see Table I) at $0<\delta<0.02$ and $d_{x^2-y^2}$-wave pairing at $0.02<\delta<0.15$ and is a normal state at $\delta>0.15$.

quasiparticles, whose positions are determined by the crossing of the lines $\cos k_x=\cos k_y$ and the Fermi surface, similar to those obtained in the t-J model. Note that the d-wave pairing has been previously found to be stable against the weak frustrations, as studied by various authors[15,16,19] on anisotropic triangular lattices. At large $|t'/t|$, the ground state has an s-s wave pairing symmetry with $\Delta_x=\Delta_y$ and $\Delta_a=\Delta_b$. In that state, the relative phase between Δ_a and Δ_x is π. Between the above two regions, there is a small parameter region around $|t'/t|=1$, where the ground state has a $d+id$ pairing symmetry at small δ and a $d+is$ phase at larger δ for negative t'/t. In both $d+id$ and $d+is$ states, the relative phases between Δ_a and Δ_x are close to $\pi/2$ and are weakly dependent of δ, and the time-reversal symmetry is spontaneously broken. We note that Hamiltonian (1) is asymmetric with respect to positive and negative values of t'/t, which is reflected in our phase diagram. Similar to the case in the t-J model, the particle-particle mean-field amplitude Δ disappears at large δ, and the ground state becomes a normal metal. The details of the phase boundaries between the superconducting and normal metallic states will be elaborated below. We also note that in the limit $|t'/t|\to\infty$, the ground state becomes 1D-like.

In Fig. 3, we display the amplitudes of the mean-field parameters as functions of δ at the symmetric point $t'/t=1$. At very low hole density, the ground state has $d+id$-wave pairing symmetry, and $\Delta_a=i|\Delta_a|$, but $|\Delta_a|\ll\Delta_x$. As δ increases, the ground state becomes a d wave, and $\Delta_a=\Delta_b$ vanishes. In comparison with the mean-field amplitudes found in the t-J model, ξ_x is similar and insensitive to δ, but Δ_x decreases more rapidly in the checkerboard model as δ increases. The latter may be understood as the consequence of the nonzero value of ξ_a in the present case, which increases rapidly as δ increases. Note that the s-s wave state has a very close energy, although it is slightly higher than either $d+id$- or d-wave states. Recently, Poilblanc[21] performed a finite cluster exact diagonalization study of the t-J model on a checkerboard lattice. Some exotic states for positive t are found to have $d_{x^2-y^2}$, s-s symmetries, which appear to be consistent with our results.

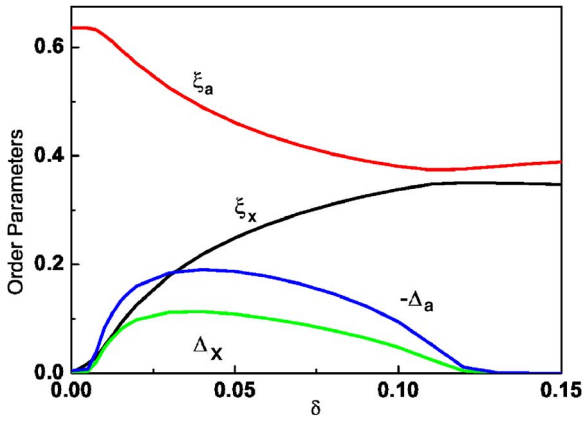

FIG. 4. (Color online) Amplitudes of the mean fields ξ and Δ as functions of δ for parameters $t=1$, $t'/t=1.1$, $J=1/3$, $J'/J=1.21$. The ground state is an s-s wave at $0.02<\delta<0.12$ and a normal state otherwise.

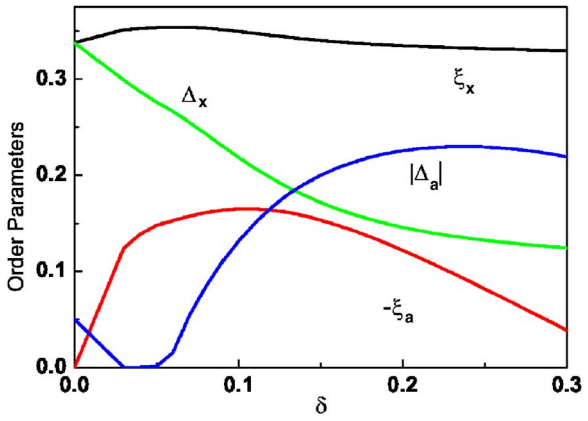

FIG. 6. (Color online). Amplitudes of mean fields ξ and Δ as functions δ for the parameters $t=1$, $J=J'=1/3$, $t'=-1$. The ground state is $d+id$ wave at $0<\delta<0.02$, d wave at $0.02<\delta<0.06$, and $d+is$ wave at $\delta>0.06$.

The mean-field amplitudes as functions of δ for the model at $t'/t=1.1$ are depicted in Fig. 4. The ground state is an s-s wave at $0.02<\delta<0.12$. The pairing amplitudes disappear around $\delta=0.12$, indicating the ground state to be a normal metallic state at $\delta>0.12$. As we can see, the correlations along the diagonal directions ($\hat{a}$ and $\hat{b}$) become more important than those along $\hat{x}$ and $\hat{y}$ directions at $t'/t>1$. Note that the results near the half-filled need to be cautious. At the half-filling, the mean-field ground state has only nonzero values of ξ_a and ξ_b, indicating that the state is a collection of the decoupled chains along the directions of $\hat{a}$ and $\hat{b}$. This may attribute to the poor Gutzwiller approximation on 1D systems.[23]

In Figs. 5 and 6, we show typical δ dependence of the mean-field amplitudes for parameters $t'/t<0$. In this case, ξ_a and ξ_b have the opposite sign with ξ_x or ξ_y. At small value of $|t'/t|$, the ground state is a d-wave state, and the amplitudes of the mean fields are illustrated in Fig. 5 for $t'/t=-0.5$. In that state, $\Delta_a=\Delta_b=0$ and $\xi_a=\xi_b$ are small and change sign at $\delta>0.2$. Interestingly, Δ_x decreases much slower as δ increases, in comparison with that in the t-J model. This suggests that the superconducting state may extend to a much larger hole density.

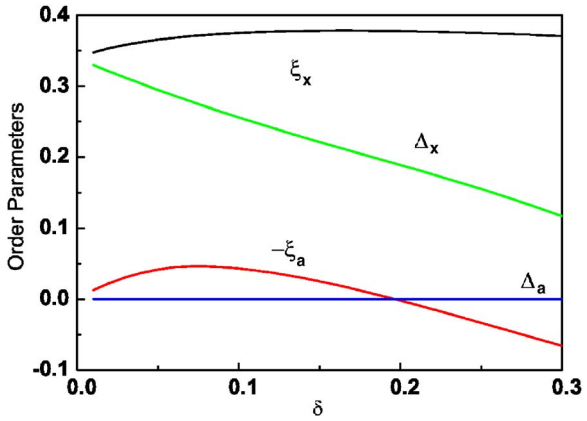

FIG. 5. (Color online) Amplitudes of mean fields ξ and Δ as functions δ in the case of $t=1$, $J=1/3$, $t'/t=-0.5$, $J'/J=0.25$. $\Delta_a=\Delta_b=0$, and the ground state has a d-wave pairing symmetry (see Table I).

In Fig. 6, we plot the mean-field amplitudes for $t'/t=-1$. Away from half-filling, the amplitudes of mean fields change nonmonotonically and there exist three distinct pairing symmetries with respect to different doping levels. As hole density increases, the ground state evolves from the $d+id$-wave state ($\Delta_a=-\Delta_b=i|\Delta_a|$) to the d-wave state and to the $d+is$-wave state ($\Delta_a=\Delta_b=i|\Delta_a|$), as we can see from the figure that the amplitude of Δ_a decreases to zero around $\delta=0.02$ and arises again at $\delta=0.06$. In contrast to the $d+id$-wave state, the amplitude of $\Delta_{a(b)}$ is comparable to Δ_x in the $d+is$-wave state. In comparison with the case of positive t'/t, we note that the suppression of Δ_x becomes much slower as δ increases and the superconductivity appears more favored for negative t'/t. This result is in agreement with previous studies for a t-J model on a triangular lattice.[15,16] An intuitive physical understanding of such effect can be given as follows: for positive t'/t, the t' and t terms in kinetic energy match quite well, so that the t' term may enhance the kinetic energy (make it lower), hence suppressing the pairing amplitude; for negative t'/t, the t' term may introduce frustration in kinetic energy, hence enhancing the pairing amplitude. The situation here is similar to that in cuprates, where the positive t'/t case corresponds to the electron-doped system while the negative t'/t case corresponds to the hole-doped system. It is well known that the hole-doped system has a higher transition temperature while the electron-doped system has a lower one and a substantial region in doping with antiferromagentic long-range order which we have not considered in the present paper for simplicity.

IV. SUMMARY

We have applied the renormalized mean-field theory to study the Gutzwiller projected BCS ground state for the t-t'-J-J' model on a highly frustrated checkerboard lattice.

As charge carriers are introduced, the half-filled Mott insulator is evolved to resonating valence bond superconducting states, with four types of pairing symmetries depending on the hole density and the parameter t'/t. We have found that the $d_{x^2-y^2}$-symmetry state previously obtained for the t-J model is most stable in a large parameter region for small values of $|t'/t|$. In this region, the d-wave pairing order parameter is suppressed for positive t'/t and enhanced for negative t'/t. At large value of $|t'/t|$, the ground state is found to be the so-called s-s wave. Around $|t'/t|=1$, we have found the time-reversal symmetry broken states. $d+id$- and $d+is$-symmetry states are the most stable. The appearance of the exotic superconducting pairing symmetry in the t-t'-J-J' model on a checkerboard lattice may be viewed as the interplay between geometrical frustration and strong electron correlation. Our results may shed light on the understanding of the pairing symmetry features of highly frustrated systems.

ACKNOWLEDGMENTS

H.-X.H. thanks X. Wan for numerical assistance. Y.C. would like to thank Z. D. Wang and Q. H. Wang for helpful discussions. This research was supported by the RGC grants (HKU-3/05C, HKU7057/04P, and HKU7012/06P) of Hong Kong SAR government, seed funding grant from the University of Hong Kong, Faculty Development Fund of the Faculty of Science at HKU, Shanghai Education Development Foundation, and NSF of China Nos. 10225419 and 10674117.

APPENDIX

In this appendix, we present detailed calculations of the mean-field theory. We first diagonalize mean-field Hamiltonian (6) on the checkerboard lattice. We carry out the Fourier transformation of electron operator in the two sublattices A and B,

$$c_{i\sigma}=\sum_{\vec{k}}\frac{1}{\sqrt{N}}a_{\vec{k}\sigma}\exp(i\vec{k}\cdot\vec{r}_i),\quad i\in A, \tag{A1}$$

$$c_{i\sigma}=\sum_{\vec{k}}\frac{1}{\sqrt{N}}b_{\vec{k}\sigma}\exp(i\vec{k}\cdot\vec{r}_i),\quad i\in B. \tag{A2}$$

The summation over $\vec{k}=(k_x,k_y)$ runs in the reduced Brillouin zone. N is the number of sites in each sublattice. By using a spinor representation, the effective Hamiltonian can be written as

$$H_{eff}=\sum_{\vec{k}}\eta_{\vec{k}}^{\dagger}M_{\vec{k}}\eta_{\vec{k}}+\text{const}, \tag{A3}$$

where $\eta_{\vec{k}}^{\dagger}=(a_{\vec{k}\uparrow}^{\dagger},b_{\vec{k}\uparrow}^{\dagger},a_{-\vec{k}\downarrow},b_{-\vec{k}\downarrow})$ and the matrix $M_{\vec{k}}$ reads

$$M_{\vec{k}}=\begin{pmatrix}A(\vec{k})-\mu & B(\vec{k})\\ B^{\dagger}(\vec{k}) & -A(\vec{k})+\mu\end{pmatrix}, \tag{A4}$$

where both $A(\vec{k})$ and $B(\vec{k})$ are 2×2 matrices whose elements are given by

$$A_{11}=-\left(2g_t t'+\frac{3}{4}g_s J'\xi_a\right)\cos k_a,$$

$$A_{22}=-\left(2g_t t'+\frac{3}{4}g_s J'\xi_b\right)\cos k_b,$$

$$A_{12}=A_{21}=-2g_t t(\cos k_x+\cos k_y)-\frac{3}{4}g_s J(\xi_x\cos k_x+\xi_y\cos k_y),$$

$$B_{11}=\frac{3}{4}g_s J'\Delta_a\cos k_a,$$

$$B_{22}=\frac{3}{4}g_s J'\Delta_b\cos k_b,$$

$$B_{12}=B_{21}=\frac{3}{4}g_s J(\Delta_x\cos k_x+\Delta_y\cos k_y),$$

with $k_\tau=\vec{k}\cdot\vec{\tau}$. The matrix $M_{\vec{k}}$ can be diagonalized by employing a unitary transformation as

$$[\gamma_{\vec{k}\uparrow}^{1\dagger},\ \gamma_{\vec{k}\uparrow}^{2\dagger},\ \gamma_{-\vec{k}\downarrow}^{1},\ \gamma_{-\vec{k}\downarrow}^{2}]=[a_{\vec{k}\uparrow}^{\dagger},\ b_{\vec{k}\uparrow}^{\dagger},\ a_{-\vec{k}\downarrow},\ b_{-\vec{k}\downarrow}]\times\begin{bmatrix}u_1^1 & u_1^2 & -v_2^{1*} & -v_1^{2*}\\ u_2^1 & u_2^2 & -v_2^{1*} & -v_2^{2*}\\ v_1^1 & v_1^2 & u_1^{1*} & u_1^{2*}\\ v_2^1 & v_2^2 & u_2^{1*} & u_2^{2*}\end{bmatrix},$$

where the $\vec{k}$ dependence of u_i^n and v_i^n are implied. The matrix element u and v satisfy the following conditions:

$$\sum_i u_i^1 u_i^{2*}+v_i^1 v_i^2=0,\quad \sum_i -u_i^1 v_i^2+v_i^1 u_i^2=0,$$

$$\sum_i u_1^n u_2^{n*}+v_1^{n*}v_2^n=0,\quad \sum_i u_1^n v_2^{n*}-u_1^n v_2^n=0.$$

In terms of u's and v's, the self-consistent equations for eight mean fields and the hole density are given by

$$\xi_{x(y)}=\frac{2}{N}\sum_{k,n}[f u_1^{n*}u_2^n+(1-f)v_1^n v_2^{n*}]\cos k_{x(y)},$$

$$\xi_a=\frac{2}{N}\sum_{k,n}[f|u_1^n|^2+(1-f)|v_1^n|^2]\cos k_a,$$

$$\xi_b=\frac{2}{N}\sum_{k,n}[f|u_2^n|^2+(1-f)|v_2^n|^2]\cos k_b,$$

$$\Delta_{x(y)}=\frac{2}{N}\sum_{k,n}[(1-f)u_1^n v_2^{n*}-f v_1^{n*}u_2^n]\cos k_{x(y)},$$

$$\Delta_a = \frac{2}{N}\sum_{k,n} (1-2f) u_1^n v_1^{n*} \cos k_a,$$

$$\Delta_b = \frac{2}{N}\sum_{k,n} (1-2f) u_2^n v_2^{n*} \cos k_b,$$

$$1-\delta = \frac{2}{N}\sum_{k,n} f|u_2^n|^2 + (1-f)|v_2^n|^2,$$

where the band index n runs over 1, 2 and f is the Fermi distribution function $f(E_n)$ which is the step function at zero temperature. The diagonalization of $M_{\tilde{k}}$ and the self-consistent equations are carried out numerically to obtain the phase diagram and the results reported in the text.

[1] H. T. Diep, *Frustrated Spin Systems* (World Scientific, Singapore, 2004).
[2] H. Aoki, J. Phys.: Condens. Matter **16**, V1 (2004).
[3] P. W. Anderson, Science **235**, 1196 (1987).
[4] N. Read and S. Sachdev, Phys. Rev. Lett. **62**, 1694 (1989).
[5] K. Takada, H. Sakurai, E. Takayama-Muromachi, F. Izumi, R. A. Dilanian, and T. Sasaki, Nature (London) **422**, 53 (2003).
[6] Y. Shimizu, K. Miyagawa, K. Kanoda, M. Maesato, and G. Saito, Phys. Rev. Lett. **91**, 107001 (2003).
[7] P. Mendels, A. Keren, L. Limot, M. Mekata, G. Collin, and M. Horvatic, Phys. Rev. Lett. **85**, 3496 (2000).
[8] S. Yonezawa, Y. Muraoka, Y. Matsushita, and Z. Hiroi, J. Phys.: Condens. Matter **16**, L9 (2004).
[9] Y. Kasahara, Y. Shimono, T. Shibauchi, Y. Matsuda, S. Yonezawa, Y. Muraoka, and Z. Hiroi, Phys. Rev. Lett. **96**, 247004 (2006).
[10] S. Fujimoto, Phys. Rev. Lett. **89**, 226402 (2002); Phys. Rev. B **67**, 235102 (2003).
[11] R. R. P. Singh, O. A. Starykh, and P. J. Freitas, J. Appl. Phys. **83**, 7387 (1998).
[12] O. Tchernyshyov, O. A. Starykh, R. Moessner, and A. G. Abanov, Phys. Rev. B **68**, 144422 (2003).
[13] M. Hermele, M. P. A. Fisher, and L. Balents, Phys. Rev. B **69**, 064404 (2004).
[14] O. A. Starykh, A. Furusaki, and Leon Balents, Phys. Rev. B **72**, 094416 (2005).
[15] M. Ogata, J. Phys. Soc. Jpn. **72**, 1839 (2003).
[16] B. Kumar and B. S. Shastry, Phys. Rev. B **68**, 104508 (2003); G. Baskaran, Phys. Rev. Lett. **91**, 097003 (2003).
[17] C. H. Chung and Y. B. Kim, Phys. Rev. Lett. **93**, 207004 (2004).
[18] S. S. Lee and P. A. Lee, Phys. Rev. Lett. **95**, 036403 (2005).
[19] J. Y. Gan, Y. Chen, and F. C. Zhang, Phys. Rev. B **74**, 094515 (2006).
[20] A. Lauchli and D. Poilblanc, Phys. Rev. Lett. **92**, 236404 (2004).
[21] D. Poilblanc, Phys. Rev. Lett. **93**, 197204 (2004).
[22] D. Poilblanc, A. Lauchli, M. Mambrini, and F. Mila, Phys. Rev. B **73**, 100403(R) (2006).
[23] F. C. Zhang, C. Gros, T. M. Rice, and H. Shiba, Supercond. Sci. Technol. **1**, 36 (1988).
[24] P. W. Anderson, P. A. Lee, M. Randeria, T. M. Rice, N. Trivedi, and F. C. Zhang, J. Phys.: Condens. Matter **24**, R755 (2004).
[25] M. C. Gutzwiller, Phys. Rev. **137**, A1726 (1965).
[26] D. Vollhardt, Rev. Mod. Phys. **56**, 99 (1984).
[27] G. Kotliar and J. Liu, Phys. Rev. B **38**, 5142 (1988).